2 Finite element Legendre wavelets Galerkin approach to inward solidification in simple body under most generalized boundary condition

2.1 Introduction

Modern technology demands to prepare a high strength material with exceptionally superior tensile properties, but at low cost. The most attractive method of producing such materials is through unidirectional solidification. A desired type of microstructure can be obtained by controlling the freezing conditions and adding a small quantity of impurity elements. The microstructure of eutectic alloys also depends on the rate of freezing. When $ZrO_2 - MgO$ eutectic freezes (Kennard *et al.* (1974)) at growth rate 8.9 cm/hr, cellular structure is formed whereas at growth rate 1 cm/hr, the microstructure of $ZrO_2 - MgO$ eutectic is fully aligned with MgO rods in a cubic ZrO_2 matrix. At slow growth rates $Al_2O_3 - UO_2$ forms a rod eutectic, but at higher growth rates, the UO_2 rods tend to form a lamellar structure. The rate of freezing which controls the structure depends on a number of parameters. In order to determine the effect of these parameters on the rate of freezing, it is desirable to develop a generalized theoretical model which may predict transport phenomena during solidification.

Industrial thermal processes where energy availability and its utilization are not coincident require a means of matching the use of energy with its availability. One can include the sensible and latent heat concepts of energy storage. Because of the large storage capacity and constant charge and discharge temperature, the

latent heat concept is more attractive. The cool thermal storage systems include liquid-solid phase change materials encapsulated in containers of different geometrical shape understanding the thermal behaviour during phase change in the container, it is important to design efficient storage systems. The solidification which has immense technological importance mathematically occurs in a class of problems commonly known as moving boundary problems. The study of these problems is not simple as the freezing front is not known in advance and along the freezing front temperature gradients are discontinuous. A good account of the analytical and numerical solutions of these problems can be found in a book by Crank (1984). Several researchers (Tien and Geiger (1967); Carslaw and Jaegar (1959); Ozisik (1993); Hill (1987); Viskanta (1988); Barry and Goodling (1987)) also studied solidification problems from a heat transfer point of view. None of these authors studied inward solidification within a container filled with melt of phase change material. Goodling and Khader (1974) obtained numerical solutions for one phase one-dimensional inward solidification problem with radiation-convection boundary condition. Gupta and Arora (1987) obtained analytical and numerical solutions of inward spherical solidification of a superheated melt with the radiative-convective heat transfer and density jump at the freezing front. Yan and Huang (1974) used a perturbation solution for one-phase slab problem. Shih and Chou (1971) presented an iterative method of successive approximations to study the solidification process inside spherical geometry. Rai and Rai (2003) used finite difference method to solve a problem of inward solidification of slabs, cylinder and sphere. The solution of this problem is found in terms of eigenvalues and spectral component of the operator. Hill and Kucera (1983) developed a semi-analytical method to study the solidification inside spherical containers taking into account the effects of heat radiation on the container surface. They estimated the time for complete solidification of the sphere. Ismail and Henriquez (2000) presented a numerical study of the solidification of phase change material (PCM) enclosed in a spherical shell. Bilir and Zafer (2005) investigated the inward solidification problem of PCM encapsulated in cylindrical or spherical containers. Chan and Tan (2006) carried out an experimental study of the solidification of an n- Hexadecane inside a spherical container. In case

of inward solidification, the effect of shape factor of container containing melt and the condition posed on boundary are not discussed in detail.

In this chapter, a model describing solidification of melt within a container of geometrical configuration likes slab, circular cylinder or sphere when its surface subjected to the most generalized boundary conditions is presented. Initially, the melt is at its freezing temperature. Several assumptions have to be taken at the surfaces from which solidification commences. Such as constant/time varying container surface temperature, constant/time varying heat flux at the container surface and constant convective heat transfer coefficient between the container surface and surrounding medium. To solve this model, we have used finite element Legendre wavelets Galerkin method (FELWGM) for finding the temperature and position of moving interface. Furthermore, the effect of parameters such as Predvoditelev number, Kirpichev number, Biot number and Stefan number on moving layer thickness is discussed in detail.

2.2 Formulation of Mathematical Model

A liquid phase change material contained either in a finite slab of thickness $2R$ or a cylinder or a sphere of diameter $2R$ is initially at its freezing temperature T_f. After time $t > 0$, the boundary is cooled by imposing on it the boundary condition of first kind or second kind or third kind. Namely, one might assume either a constant temperature $T_w < T_f$ (subscript w stands for wall and f stands for freezing) or a constant heat flux q or a constant heat transfer coefficient α. It is supposed that: (i) heat transfer is only in the r- direction; (ii) the container walls are so thin and of a low conductive material that the thermal resistance through the walls is negligible, the fact which is confirmed experimentally by Tan and Leong (1999); (iii) mass densities of solid and liquid phases are equal. The melt freezes inward and the solidification shell grow in a symmetric manner. The finite region is divided into two regions separated by solidification front $r = s(t)$. The first region $s(t) < r < R$ in frozen form while the region $0 < r < s(t)$ in liquid form. The dynamics of

freezing can be described by the following equations:

$$\frac{\partial T}{\partial t} = \frac{a}{r^{\Gamma}} \frac{\partial}{\partial r} \left(r^{\Gamma} \frac{\partial T}{\partial r} \right), \; s(t) < r < R, \; t > 0, \tag{2.1}$$

T is the temperature, a the thermal diffusivity, r the position of the solidification material, and $\Gamma = 0, 1, 2$ for a slab, cylinder and spherical configuration respectively. The initial condition and associated boundary conditions are

$$T(r, t) = T_f, \;\; t = 0, \tag{2.2}$$

$$A_0 \frac{\partial T}{\partial r} + B_0 T = f_0(t), \; r = R, \; t > 0. \tag{2.3}$$

Where

1. $A_0 = 0, \;\; B_0 = 1, \;\; f_0(t) = T_w,$
2. $A_0 = -K_0, \;\; B_0 = 0, \;\; f_0(t) = q,$
3. $A_0 = -K_0, \;\; B_0 = \alpha, \;\; f_0(t) = -\alpha T_{\infty}.$

are defined in first, second and third kind of boundary condition respectively. The energy balance at the solid-liquid interface is

$$\frac{d(s(t))}{dt} = \frac{K}{\rho L} \frac{\partial T}{\partial r}, \;\; r = s(t), \tag{2.4}$$

$$s(0) = 0, \;\; r = R, \tag{2.5}$$

$$T(r, t) = T_f, \;\; r = s(t), \tag{2.6}$$

where ρ is the density, L denote the latent heat of fusion and $s(t)$ denote the thickness of moving layer.

2.2.1 Dimensionless Analysis

Introducing the dimensionless variables

$$x = \frac{r}{R}, \;\; Ste = \frac{c \triangle T}{L}, \;\; \lambda = \frac{s(t)}{R}, \;\; Fo = \frac{at}{R^2}, \;\; \theta = \frac{(T - T_0)}{\triangle T}. \tag{2.7}$$

where

$$\triangle T = T_f - T_w,\ T_0 = T_w, \tag{2.8}$$

$$\triangle T = \frac{ql}{K},\ T_0 = T_f - \triangle T, \tag{2.9}$$

$$\triangle T = T_f - T_\infty,\ T_0 = T_\infty, \tag{2.10}$$

in first, second and third kind of boundary conditions respectively. Further

$$A^{'} = \frac{A_0}{R},\ B^{'} = B_0,\ \theta_c(Fo) = \frac{f_0(t) - B_0 T_0}{\Delta T}.$$

The system of Eqs. (2.1)-(2.5) reduce into the dimensionless form as follows:

$$\frac{\partial \theta}{\partial Fo} = \frac{1}{x^\Gamma}\frac{\partial}{\partial x}\left(x^\Gamma \frac{\partial \theta}{\partial x}\right),\ \lambda(Fo) < x < 1, Fo > 0, \tag{2.11}$$

$$A^{'}\frac{\partial \theta}{\partial x} + B^{'}\theta = \theta_c(Fo),\ x = 1, \tag{2.12}$$

$$\theta(x, Fo) = 1,\ x = \lambda, \tag{2.13}$$

$$\frac{d\lambda}{dFo} = Ste\frac{\partial \theta}{\partial x},\ x = \lambda, \tag{2.14}$$

$$\lambda(0) = 0, \tag{2.15}$$

$$\theta(x, 0) = 1. \tag{2.16}$$

Replacing the domain $[0, 1] \times [0, \infty]$ by a rectangular grid of points (x_i, Fo). We first deal with the discretization in the space variable by using central differences, Eqs.(2.11 - 2.13) and Eq. (2.16) can be written in vector matrix form as follows:

$$\frac{d\bar{\theta}}{dFo} = A\bar{\theta} + B, \tag{2.17}$$

and initial condition is

$$\bar{\theta}(0) = \begin{bmatrix} 1 & 1 & \cdots & \cdots & 1 \end{bmatrix}^T. \tag{2.18}$$

Here

$$\bar{\theta}(Fo) = \begin{bmatrix} \theta_1 & \theta_2 & \cdots & \cdots & \theta_k \end{bmatrix}^T,$$

where,

$$\theta_i(Fo) = \theta(x_i, Fo),$$

$$A = \frac{1}{2h^2 Ste}\begin{pmatrix} \frac{13A'\left(\frac{\Gamma h}{x_1}-2\right)}{20hB'-21A'}-4 & \frac{17A'\left(\frac{\Gamma h}{x_1}-2\right)}{20hB'-21A'}+\left(\frac{\Gamma h}{x_1}+2\right) & \frac{-9A'\left(\frac{\Gamma h}{x_1}-2\right)}{20hB'-21A'} & \cdots & 0 \\ \left(-\frac{\Gamma h}{x_2}+2\right) & -4 & \left(\frac{\Gamma h}{x_2}+2\right) & \cdots & \\ 0 & \left(-\frac{\Gamma h}{x_3}+2\right) & -4 & \left(\frac{\Gamma h}{x_3}+2\right) & \cdots \\ 0 & 0 & \left(-\frac{\Gamma h}{x_4}+2\right) & -4 & \cdots \\ 0 & 0 & \cdots & \cdots & 0 \\ 0 & \cdots & \cdots & \cdots & 0 \\ 0 & \cdots & \cdots & \cdots & 0 \\ 0 & \cdots & \cdots & \cdots & 0 \\ 0 & \cdots & \left(-\frac{\Gamma h}{x_{k-1}}+2\right) & -4 & \left(\frac{\Gamma h}{x_{k-1}}+2\right) \\ 0 & \cdots & 0 & \left(-\frac{\Gamma h}{x_k}+2\right) & -4 \end{pmatrix},$$

and

$$B = \frac{1}{2h^2 Ste}\left[\begin{array}{cccccccc} \frac{20h\left(\frac{-\Gamma h}{x_1}+2\right)\theta_c(Fo)}{20hB'-21A'} & 0 & 0 & \cdots & \cdots & \cdots & 0 & \left(\frac{\Gamma h}{x_k}+2\right) \end{array}\right]^T.$$

2.3 Finite Element Legendre Wavelets Galerkin Method

To solve the differential Eq. (2.17) under initial condition defined in Eq. (2.18), let us assume that

$$\frac{d\bar{\theta}}{dFo} = X\psi, \tag{2.19}$$

where X is unknown matrix of order $2^{k-1}M \times 2^{k'-1}M'$ $(M' \leq M, k' \leq k)$ and ψ is a vector of Legendre wavelets of order $2^{k-1}M' \times 1$ given as follow:

$$\begin{aligned} \psi\,(Fo) = \quad & [\psi_{10}(Fo), \psi_{11}(Fo), \ldots, \psi_{1M-1}(Fo), \psi_{20}(Fo), \ldots, \psi_{2M-1}(Fo), \ldots, \\ & \psi_{2^{k-1}0}(Fo)\psi_{2^{k-1}1}(Fo), \ldots, \psi_{2^{k-1}M-1}(Fo)]^T. \end{aligned} \tag{2.20}$$

The elements of ψ are defined in Eq. (1.87). Integrating the Eq. (2.19) from 0 to Fo and using initial condition and Eq. (1.92), we get

$$\bar{\theta}(Fo) = \bar{\theta}(0) + XP\psi, \tag{2.21}$$

where P is operational matrix of integration of order $2^{k-1}M \times 2^{k-1}M$ defined in Eq. (1.93). Substituting the value of $\theta(Fo)$ in the differential Eq. (2.17), we get

$$X\psi = A(\theta(0) + XP\psi) + B, \tag{2.22}$$

$$AXP\psi - X\psi + A\theta(0)d^T\psi + Bd^T\psi = 0, \tag{2.23}$$

where d is a vector coefficient determine by $< \psi_{nm}, d^T \psi(x) > = < \psi_{nm}, 1 >$, where ψ_{nm} is defined in Eq. (1.87). The Eq. (2.23) reduces in the form of

$$AXP - X + (A\theta(0) + B)d^T = 0. \tag{2.24}$$

Let $N = (A\theta(0) + B)d^T$, the above system reduces to

$$AXP - X + N = 0. \tag{2.25}$$

We look for the generalized time Fo in which the interface moves a distance $\lambda(Fo)$. The region $(1 - \lambda, 1)$ is divided into k equal subregions. Assuming a fix $Fo^* = Fo > 0$, the elements of matrix X are computed by solving the Sylvester Eq. (2.25). The interface condition Eq. (2.14) is used to evaluate the generalized time Fo^*. By replacing the space derivative by its average value and then integrating with respect to Fo from 0 to Fo, we obtain

$$\lambda(Fo) = \frac{1}{20h} \int_0^{Fo} (21 - 13\theta_k - 17\theta_{k-1} + 9\theta_{k-2}) dFo. \tag{2.26}$$

2.4 Numerical Computation and Discussion

The above solutions are of interest as they describe the inward solidification process of melt in different geometries such as slab, circular cylinder or sphere when surface subjected under most generalized boundary condition. To analyze the solution, we consider particular cases of technical importance. In general, it is categorized into the following three different modalities:

Case 1: The surface is subjected to boundary condition of first kind. In this case, we take

$$A^{'} = 0,\ B^{'} = 1,\ (\mathrm{I})\ \theta_c(Fo) = 0,\ (\mathrm{II})\ \theta_c(Fo) = Pd * Fo, \tag{2.27}$$

where Pd is predvoditelev number defined as $Pd = \frac{bR^2}{a\Delta T}$.

Case 2: The second kind boundary condition consists in assigning heat flux at the surface. In this case, we take

$$A^{'} = 1,\ B^{'} = 0,\ (\mathrm{I})\ \theta_c(Fo) = 0, (\mathrm{II})\ \theta_c(Fo) = Ki(Fo) = Kie^{(-PdFo)}, \tag{2.28}$$

where Ki is Kirpichev number defined as $Ki = \frac{qR}{K\Delta T}$.

Case 3: The third kind boundary conditions generally characterize the law of convective heat transfer between the surface of a body and its surrounding for a constant heat flux. In this case, we take

$$A^{'} = 1,\ B^{'} = Bi,\ \theta_c(Fo) = 0, \tag{2.29}$$

where Bi is Biot number defined as $Bi = \frac{\alpha R}{K}$.

The computation has been made and the results are presented in tables and eighteen figures. On the figures presented in this study, only the parameters whose values different from the reference values are indicated. The selected reference values include $Pd = 1.0, Ki = 1.0, Bi = 1.0, Fo = 1.0$. The dimensionless temperature θ, at the end of solidification process, as a function of space coordinate for slab, circular cylinder and sphere for boundary condition of first, second kind are shown in Figs. (2.1), (2.2) and (2.3), (2.4) respectively. In third kind of boundary condition the temperature θ for slab, circular cylinder and sphere are shown in Table (2.1). The solid region thickness as a function of generalized time Fo for different Γ under boundary condition of first and second kind are depicted in Figs. (2.5) and (2.6) respectively. A slab takes time $Fo = 0.0578$, a circular cylinder $Fo = 0.0644$ and a sphere $Fo = 0.0736$ when surface subjected to boundary conditions of first kind. When the surface is subjected to boundary conditions of second kind, slab takes $Fo = 0.50$, cylinder takes $Fo = 0.82$ and sphere takes $Fo = 0.90$. When the surface is subjected to boundary conditions of third kind as shown in Table (2.2), slab takes time $Fo = 0.88$, cylinder takes $Fo = 0.90$ and sphere takes $Fo = 0.92$. In basic equation of heat conduction in a simple body like infinite plate, circular cylinder and sphere, the term $\frac{\partial T}{\partial t}$ represents the rate of change of temperature with respect to time and can be replaced by $\frac{\delta T_t}{t}$. Similarly, $\frac{\partial T}{\partial r}$ represents the rate of change of temperature with respect to r and can be replaced by $\frac{\delta T_R}{R}$. The term $\frac{\partial^2 T}{\partial r^2}$ is the square rate of change of T with respect to r and it can be replaced by $\frac{\delta T_R}{R^2}$, where the suffixes t and R denote the time rate and space rate change in temperature T. Therefore, heat conduction equation reduces to

$$\frac{\delta T_t}{t} = a\left(\frac{\delta T_R}{R^2} + \frac{\Gamma}{R}\frac{\delta T_R}{R}\right), \tag{2.30}$$

i.e.

$$\frac{1}{(1+\Gamma)}\frac{\delta T_t}{\delta T_R} = \frac{at}{R^2}. \tag{2.31}$$

The right hand side of this equation being dimensionless quantity called Fourier number $Fo = \frac{at}{R^2}$ Thus, the Fourier number is defined as the ratio of time rate change in temperature with the space rate change in temperature i.e.

$$Fo = \frac{1}{(1+\Gamma)}\frac{\delta T_t}{\delta T_R}. \tag{2.32}$$

Thus, the ratio of time rate change in temperature with the space rate change in temperature increases as shape factor Γ and Fourier number both increases. This ratio is highest in a sphere and lowest in a plate. The temperature in sphere is highest and lowest in plate for all type of boundary conditions. It is evident from the Figs. (2.5) and (2.6) that the moving layer thickness in slab is highest while in sphere is lowest and because of this the time taken for complete freezing in slab is lowest and in sphere is highest. In boundary condition of first kind as Pd increases, the solid layer thickness decreases and shown in Figs. (2.7 -2.9).

In case 2 when freezing starts due to assigning heat flux at the surface, solid layer thickness increases as Kirpichev number Ki increases as shown in Figs. (2.13 -2.15). The Kirpichev number relates the intensity of external heat transfer to the intensity of internal heat transfer. As ratio of intensity of external heat transfer to the intensity of internal heat transfer increases, Ki increases, the solid layer thickness increases as shown in Figs. (2.13 - 2.15). If Kirpichev number Ki varies with time following the exponential law $Ki(Fo) = Kie^{-PdFo}$, then solid layer thickness decreases as Pd increases as shown in Figs. (2.10 - 2.12). The Predvoditelev number Pd characterizes the discrete structure of a fluid and intensifies the additional mode of momentum transfer which takes place in such systems. The quantity $PdFo = \frac{bt}{\Delta T}$, increases with increase in time or decrease in ΔT. Thus, e^{-PdFo} decreases as ΔT decreases. Hence as Pd increases, $Ki(Fo)$ decreases and solid layer thickness decreases as shown in Figs. (2.10 - 2.12). In boundary condition of first kind too, as Pd increases, the solid layer thickness decreases as shown in Figs. (2.7 - 2.9) respectively.

In case 3, when surface subjected to boundary condition of third kind, as Biot

number increases, the temperature of solid region decreases (Table-2.1) while solid layer thickness increases (Table-2.2). The Biot number provides a way to compare the conduction resistance within a solid body with the convection resistance external to that body for heat transfer. It provides a way to use proper method of analysis for appropriate situations. The process is fastest in boundary condition of first kind in comparison to boundary condition of second and third kind. It is due to fact that in boundary condition of first kind, Bi is infinity, in boundary condition of second kind $Bi = \frac{1}{\theta}$ while in boundary condition of third kind, it is finite. The dynamics of propagation of the freezing front during the freezing process for Bi is infinite are different from those in the process with Bi is finite. In freezing process with infinite Bi, the front starts advancing into the liquid with infinite speed, where as in a freezing process with finite Bi the front starts advancing into the liquid with vanishing front speed. This is the reason why the freezing process is fastest in boundary condition of first kind in comparison to boundary condition of second and third kind. As the Stefan number increases, the dimensionless solid layer thickness increases and the time of complete solidification decreases. This time is minimum in slab and maximum in sphere. When the Stefan number decreases and approaches zero, the dimensionless solid layer thickness also decreases and tending to zero. The Stefan number signifies the importance of sensible heat relative to the latent heat. The higher value of heat capacity or higher ΔT (in boundary condition of first kind $\Delta T = T_f - T_0$, in boundary condition of second kind $\Delta T = \frac{qR}{K}$, in boundary condition of third kind $\Delta T = T_f - T_\infty$) or lower value of latent heat, the faster is the freezing process as shown in Figs. (2.16), (2.17) and (2.18) respectively. As the Stefan number increases, the time required for complete solidification decreases and approaches zero. In such situations the solidification process may be so rapid that liquid molecules have no time to rearrange themselves into the usual crystal structure and instead form an amorphous solid structure that is reminiscent of the liquid phase. For this reason solid formed from a supercooled liquid have been referred to as liquid of pause (NASA (2012)).

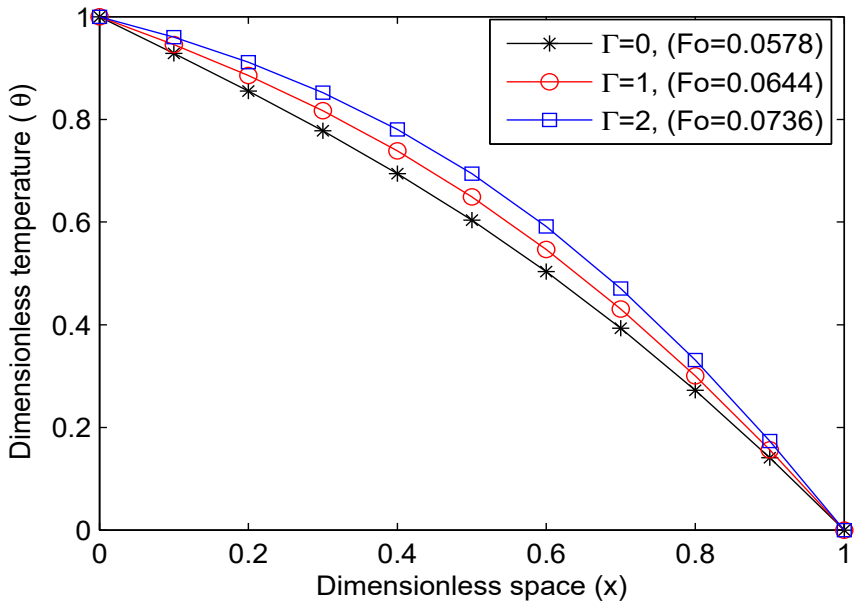

Figure 2.1: Temperature distribution in b.c. of first kind (I).

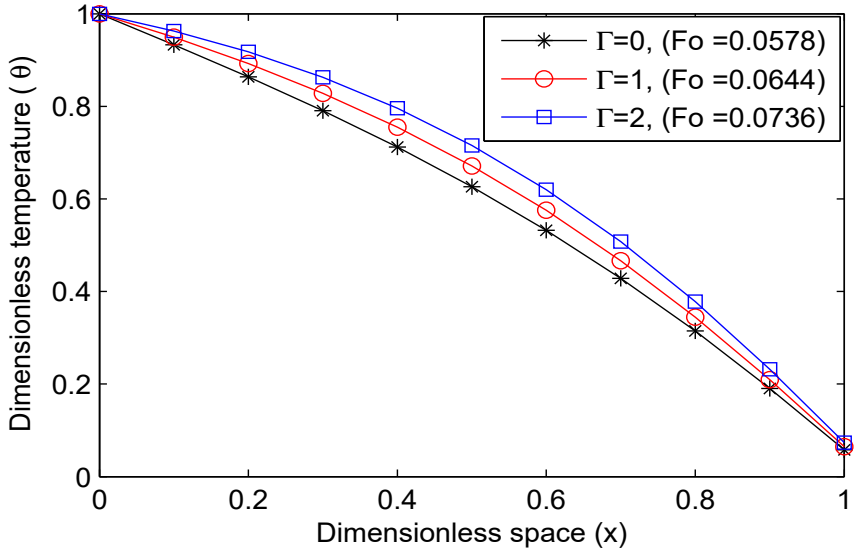

Figure 2.2: Temperature distribution in b.c. of first kind, $Pd = 1.0$ (II).

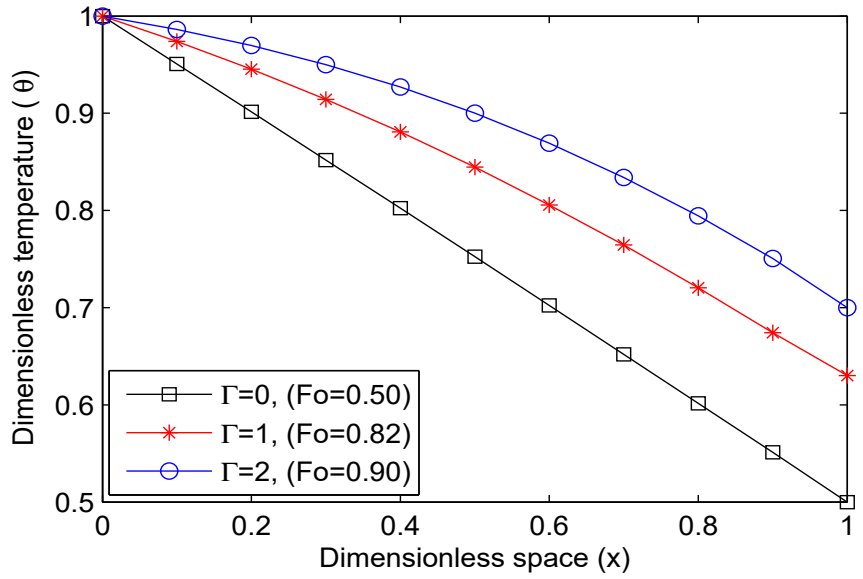

Figure 2.3: Temperature distribution in b.c. of second kind, $Ki = 1.0$ (I).

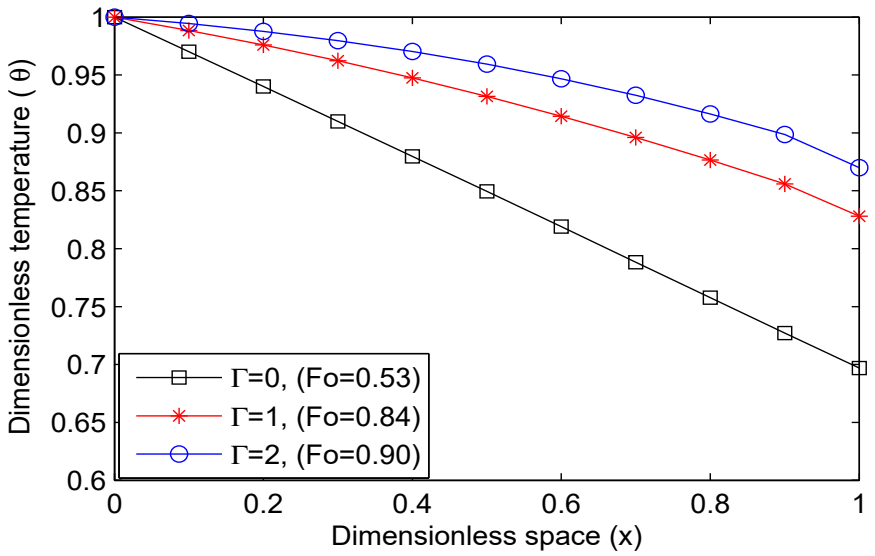

Figure 2.4: Temperature distribution in b.c. of second kind $Ki = 1.0$, $Pd = 1.0$ (II) .

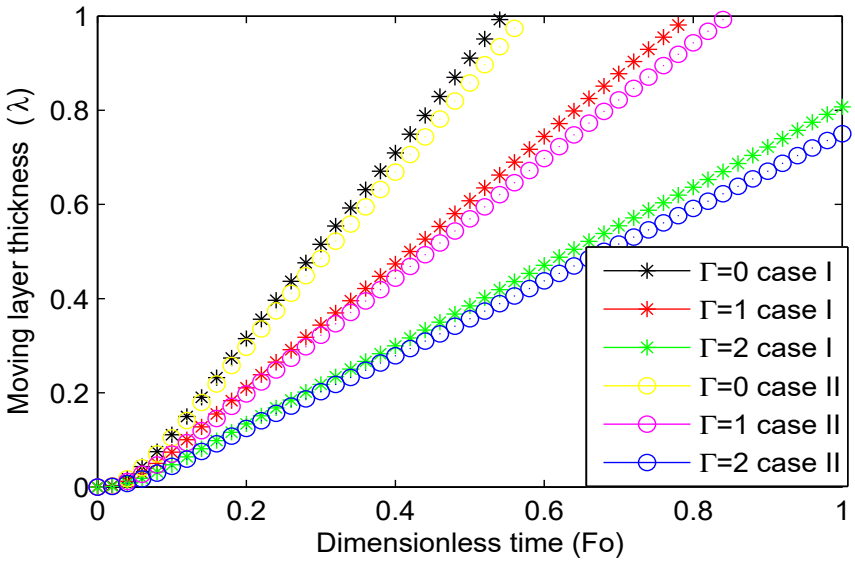

Figure 2.5: Moving layer thickness (λ) for b.c. of first kind, $Ste = 1$ (I).

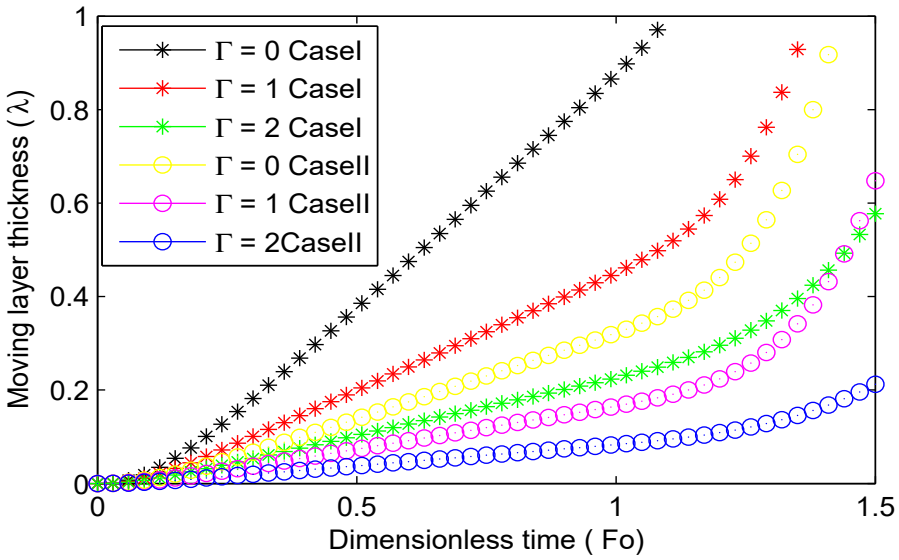

Figure 2.6: Moving layer thickness (λ) for b.c. of second kind, $Ste = 1$ (II).

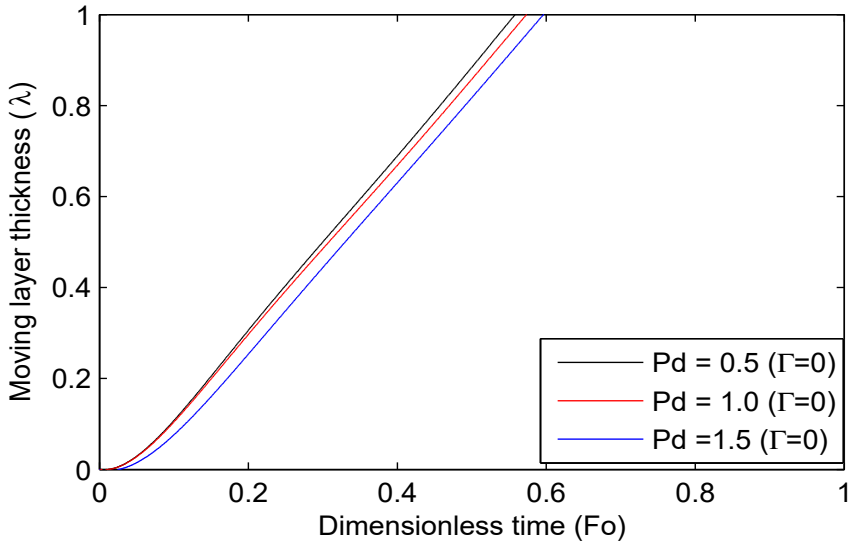

Figure 2.7: Effect of Pd on moving layer thickness (λ) for b.c. of first kind, $Ste = 1$ (II).

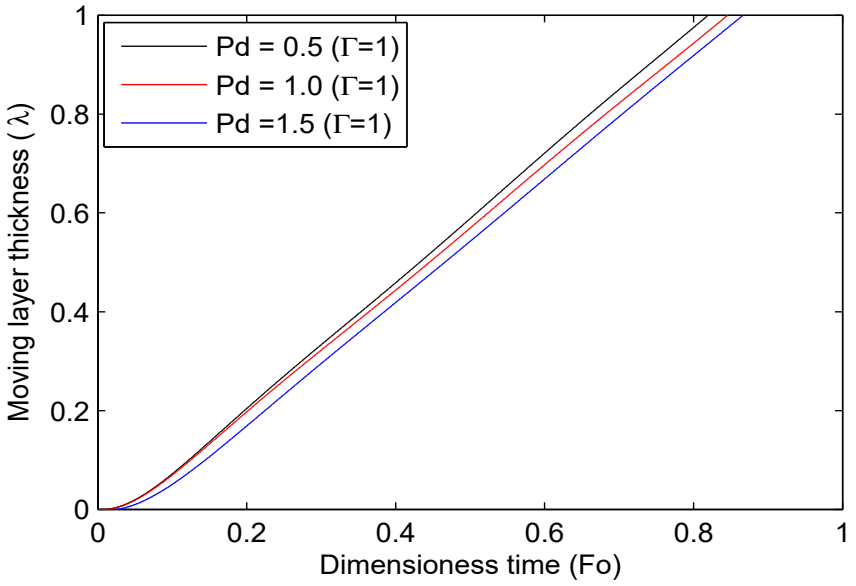

Figure 2.8: Effect of Pd on moving layer thickness (λ) for b.c. of first kind, $Ste = 1$ (II).

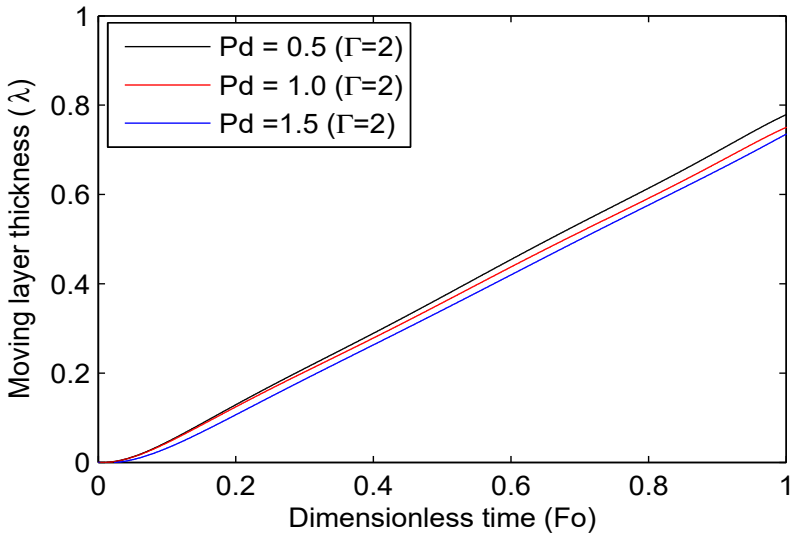

Figure 2.9: Effect of Pd on moving layer thickness (λ) for b.c. of first kind, $Ste = 1$ (I).

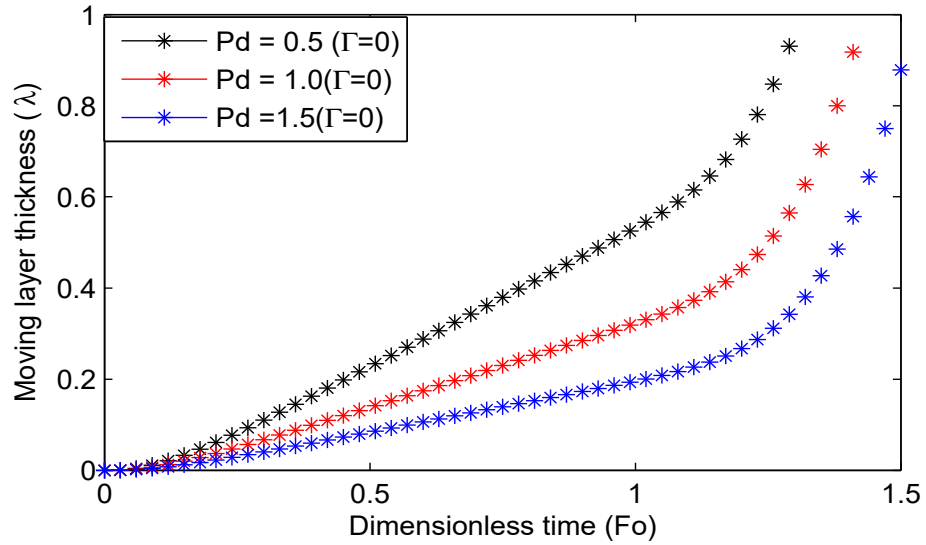

Figure 2.10: Effect of Pd on moving layer thickness (λ) for b.c. of second kind, $Ki = 1.0$, $Ste = 1$ (II).

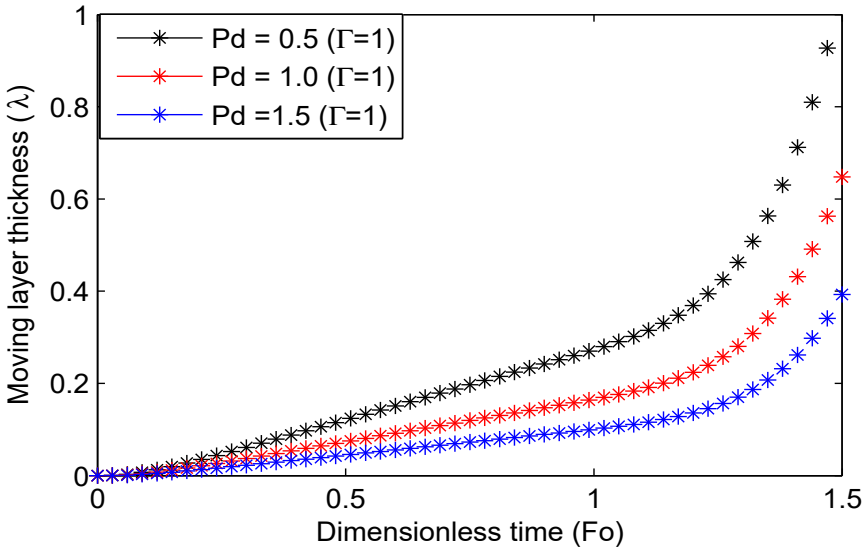

Figure 2.11: Effect of Pd on moving layer thickness (λ) for b.c. of second kind, $Ki = 1.0$, $Ste = 1$ (II).

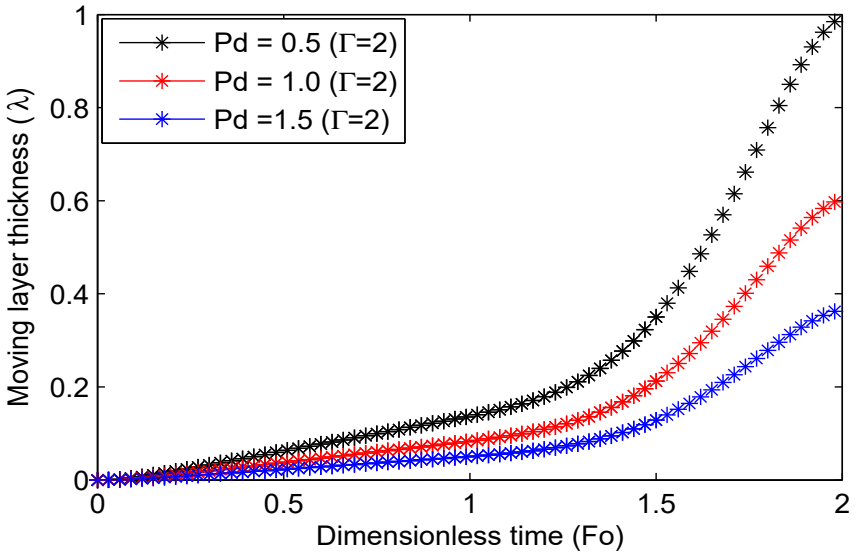

Figure 2.12: Effect of Pd on moving layer thickness (λ) for b.c. of second kind, $Ki = 1.0$, $Ste = 1$ (II).

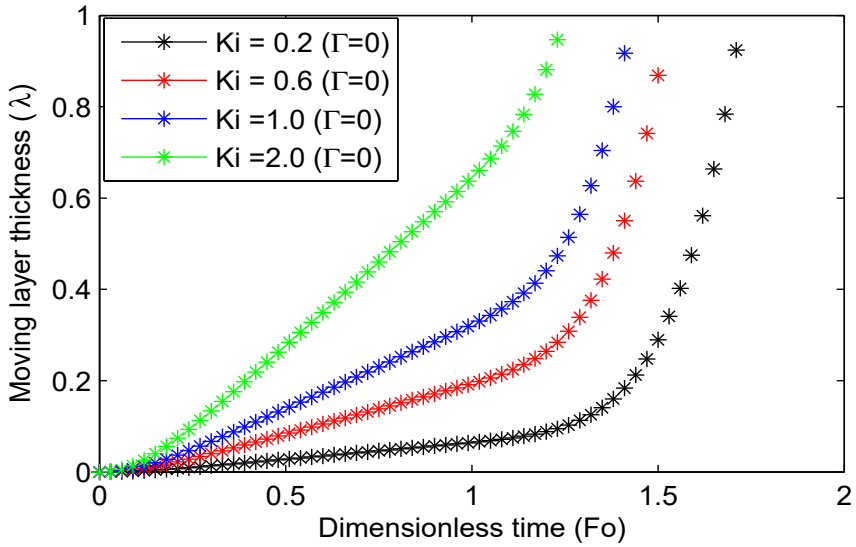

Figure 2.13: Effect of Ki on moving layer thickness (λ) for b.c. of second kind, $Pd = 1.0$, $Ste = 1$.

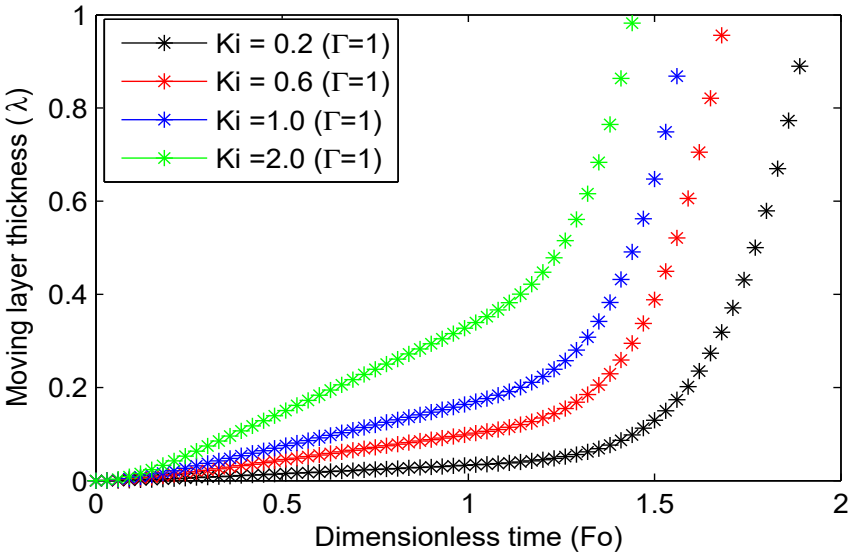

Figure 2.14: Effect of Ki on moving layer thickness (λ) for b.c. of second kind, $Pd = 1.0$, $Ste = 1$.

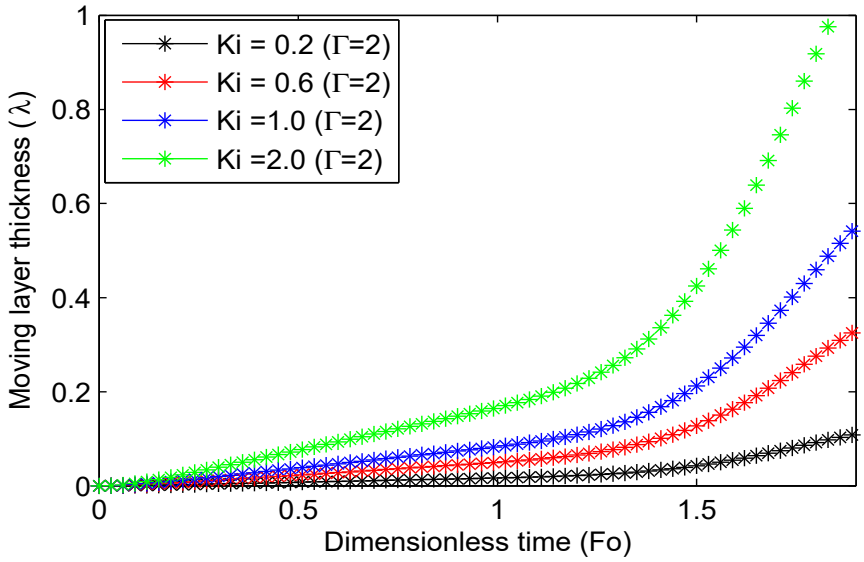

Figure 2.15: Effect of Ki on moving layer thickness (λ) for b.c. of second kind, $Pd = 1.0, Ste = 1$.

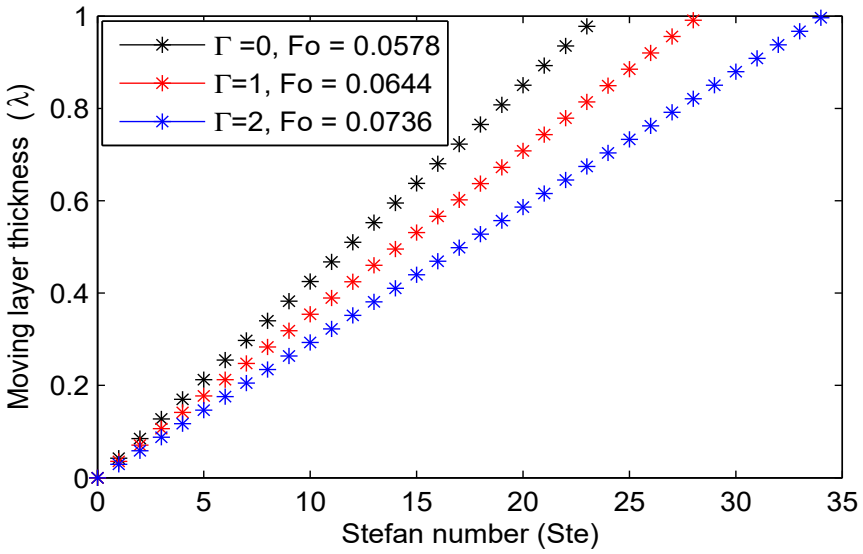

Figure 2.16: Effect of Stefan number on moving layer thickness (λ) for b.c. of first kind.

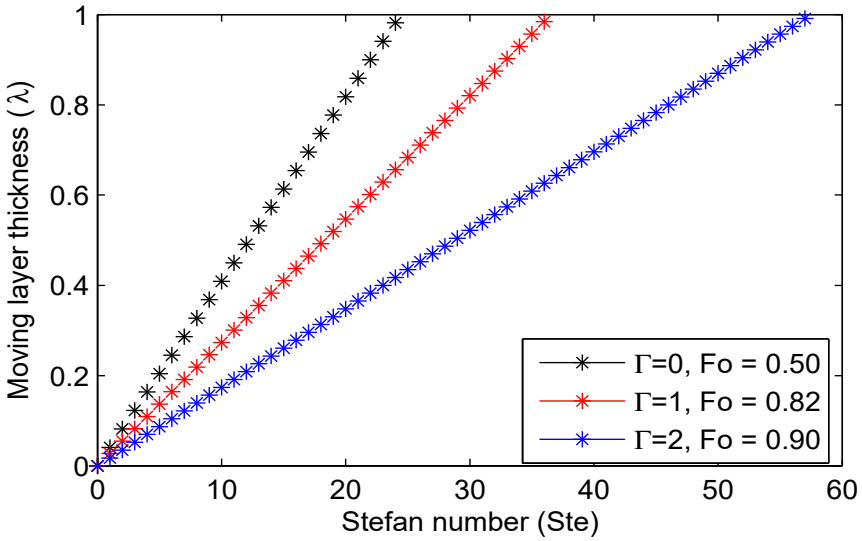

Figure 2.17: Effect of Stefan number on moving layer thickness (λ) for b.c. of second kind.

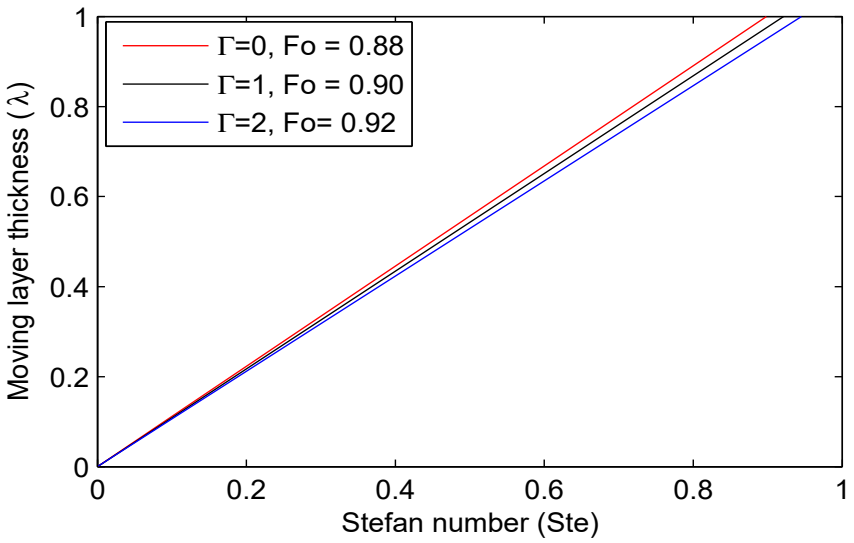

Figure 2.18: Effect of Stefan number on moving layer thickness (λ) for b.c. of third kind.

Table 2.1: Temperature (θ) for third kind of b.c.

Γ	0	1	2
F_o	0.88	0.90	0.92
x	θ	θ	θ
0	1	1	1
0.1	0.77751	0.78181	0.78613
0.2	0.55521	0.56137	0.56760
0.3	0.33328	0.33887	0.34448
0.4	0.11190	0.11449	0.11684
0.5	0.10873	0.11160	0.11528
0.6	0.10628	0.10937	0.11412
0.7	0.10454	0.10778	0.11335
0.8	0.10348	0.10683	0.11299
0.9	0.10309	0.10652	0.11305
1.0	0.09580	0.09580	0.09580

Table 2.2: Effect of B_i on moving layer thickness $\lambda, Ste = 1.0$.

Γ	0	0	0	1	1	1	2	2	2
B_i	0.2	0.4	0.6	0.2	0.4	0.6	0.2	0.4	0.6
F_o	λ	λ	λ	λ	λ	λ	λ	λ	λ
0.00	0.00000	0.00000	0.00000	0.00000	0.00000	0.00000	0.00000	0.00000	0.00000
0.01	0.22019	0.22022	0.22026	0.21465	0.21468	0.21472	0.20916	0.20920	0.20923
0.02	0.44092	0.44099	0.44106	0.42985	0.42992	0.42999	0.41890	0.41896	0.41903
0.03	0.66210	0.66221	0.66232	0.64552	0.64562	0.64572	0.62911	0.62920	0.62929
0.04	0.88366	0.88380	0.88394	0.86158	0.86170	0.86183	0.83971	0.83983	0.83995

2.5 Conclusion

A continuum model for the inward solidification of melt in different geometries under most generalized boundary condition has been presented. The finite element

Legendre wavelets Galerkin (FELWG) method has been used to obtain the solution of this moving boundary problem. It can be seen that the proposed method is efficient and accurate to determine the solution of moving boundary problem. In view of the excellent convergence of the Legendre wavelets series, only a few terms of the series are needed to give satisfactory results. The finite element method minimizes the error at each point. The exceptional accuracy prompts us to conclude that the finite element Legendre wavelets Galerkin method may be excellent alternative of other methods for solving boundary value problems containing two nonlinearities. Our simulation show that

- during solidification the dimensionless temperature is highest in sphere and lowest in slab while it is in between them in cylinder.
- the solidification process is fastest in slab and slowest in the sphere while it is in between them in cylinder.
- the solidification process is fastest in boundary condition of first kind in comparison to boundary condition of second and third kind.
- the solidification process increases as predvoditelev number Pd decreases.
- the solidification process increases as Kirpichev number Ki or Biot number Bi increases.
- the solidification process increases as Stefan number increases.